EAM
Environmental and Materials
EAM 2(2): 90-101
ISSN 3025-0277

Institute for Advanced Science, Social and Sustainable Future
MORALITY BEFORE KNOWLEDGE

The effect of acetylcholine immobilization on the electrochemical properties of thiocholine on boron-doped diamond electrode for chlorpyrifos sensor

Shafrizal Rasyid Atriardi[1,*], Adinda Muthia Hani[2], Gadis Putri[2]
[1] *Chemistry Institute for Functional Material, Pusan National University, Busan, 46241, Republic of Korea;*
[2] *Department Chemistry, Faculty of Mathematics and Natural Sciences, Universitas Indonesia, Depok, West Java 10430, Indonesia.*
*Correspondence: shafrizalrasyid@pusan.ac.kr

ABSTRACT
Background: The inhibition reactions of acetylcholinesterase (AChE) have been studied to develop chlorpyrifos biosensors. The performance of AChE, both as a free enzyme and when immobilized on avidin-functionalized magnetic beads (aMB), was evaluated for the hydrolysis of acetylthiocholine. Detection was conducted through the oxidation of thiocholine on a boron-doped diamond (BDD) electrode surface. **Methods**: The study compared the performance of free and immobilized AChE by analyzing their ability to oxidize thiocholine on the BDD electrode surface. The inhibitory effects of chlorpyrifos were assessed by determining IC10 and IC50 values for both enzyme forms. Additionally, the influence of metal ions (Fe^{2+} and Mn^{2+}) on AChE activity was investigated to evaluate interference effects. **Findings**: Free AChE demonstrated superior performance in thiocholine oxidation compared to the immobilized enzyme. In chlorpyrifos detection, free AChE exhibited a significantly lower IC10 value (3.44×10^{-6} mM) compared to immobilized AChE (12.9×10^{-6} mM), and its IC50 value (3.8×10^{-4} mM) was approximately two orders of magnitude lower than that of the immobilized AChE (5.18 mM). Furthermore, AChE exhibited resistance to metal ion interference, with signal losses of 48.7% and 40.8% in the presence of Fe^{2+} and Mn^{2+} ions, respectively. These findings indicate that the immobilization of AChE must be carefully optimized for effective sensor application. **Conclusion**: The study highlights the superior performance of free AChE in chlorpyrifos detection compared to its immobilized counterpart. Immobilization significantly affects enzyme sensitivity, resulting in higher inhibitory concentration values. Additionally, AChE demonstrated notable resistance to interference from metal ions. These results emphasize the need for careful consideration when immobilizing AChE for sensor applications. **Novelty/Originality or this article**: This study provides a detailed comparison between free and immobilized AChE in chlorpyrifos biosensing, highlighting the impact of immobilization on enzyme sensitivity and performance. The findings contribute to the development of more efficient biosensors by emphasizing the importance of optimizing enzyme immobilization strategies.

KEYWORDS: organophosphate pesticides; enzymatic sensor; magnetic beads; acetyl thiocholine; boron doped diamond.

1. Introduction

Chlorpyrifos (CO,O-diethyl O-3,5,6-trichloro-2-pyridyl phosphorothioate) is a pesticide from organophosphate group that is commonly used in agricultural activity due to its superiority against insects and worms (Mishra et al., 2021). European Union (EU) bans chlorpyrifos due to its serious risks reports especially for human being (Nandhini et al., 2021), and also causes serious problem for environment (Camacho et al., 1996; Mishra et al., 2021). Chlorpyrifos use for a long period is reported to lead to health issues not only for

Cite This Article:
Atriardi, S. R., Hani, A. M., & Putri, G. (2024). The effect of acetylcholine immobilization on the electrochemical properties of thiocholine on boron-doped diamond electrode for chlorpyrifos sensor. *Environmental and Materials*, *2*(2), 90-101. https://doi.org/10.61511/eam.v2i2.2024.1414

Copyright: © 2024 by the authors. This article distributed under the terms and conditions of the Creative Commons Attribution (CC BY) license (https://creativecommons.org/licenses/by/4.0/).

humans but also animals, especially in neurological system. It can cause dangerous symptoms, from nausea and vomiting to even death. Therefore, monitoring and action to slow down chlorpyrifos exposures in the environment is necessary (Wołejko et al., 2022).

Common conventional methods for chlorpyrifos detections and quantifications depend on chromatography techniques coupled with mass spectrometry (Van Dyk & Pletschke, 2011; Hernández et al., 2005). However, application of this method is limited due to the expensive equipment, complex procedures, time-consuming preparation, and requirement for specialized expertise (Pico et al., 2020), while biosensor employing acetylcholinesterase (AChE) as an alternative for pesticide detection due to their several advantages in terms of their economic cost and simple application (Pino et al., 2015). AChE catalyzes acetylthiocholine hydrolysis to produce thiocholine, which is electrochemically detectable on solid electrodes based on the oxidation of thiocholine.

On the other hand, boron-doped diamond (BDD) known as an alternative for solid electrodes because of its superior electrochemical properties, including a low capacitive background and very wide potential window as well as its inertness and biocompatibility due to its sp^3 hybridization (Girard et al., 2007; Waldvogel & Elsler, 2012; Chaplin et al., 2013; Vosáhlová et al., 2018; Chen et al., 2022; Raharto et al., 2023). Those properties still make BDD is the most considerable material for a sensor development. The problem in the direct immobilization of AChE on BDD surface is generally overcome by the modification of AChE with magnetic compound that can enhance the stability and sensor performance (Rachmawati et al., 2023).

In this study, chlorpyrifos biosensors is developed using a BDD electrode. To maintain the reproducibility responses of the sensor system, the AChE was immobilized with avidin-functionalized magnetic beads (aMB) with the help of biotin as a linker. The hydrolysis activity was then studied from thiocholine oxidation measurement on the BDD surface. Although higher sensitivity of free AChE than the immobilized (AChE-aMB) was observed, this study shows that AChE-aMB is a suitable method for sensor fabrication, although it is more prone to metal ion interference.

2. Methods

2.1 Materials and instruments

Most of the chemicals used in this work were supplied by Sigma Aldrich, including chlorpyrifos, acetylthiocholine iodide (ACTI), acetylcholinesterase (AChE), bovine serum albumin (BSA), phosphate buffered solution (PBS), sulfo-NHS-biotin, avidin-functionalized magnetic beads (aMB), α-alumina, sulfuric acid, sodium hydroxide, methanol, glycerol, 1-propanol, $FeCl_2.4H_2O$, and $MnCl_2.4H_2O$. All materials were used without any purification. The electrochemical behavior was studied with a potentiostat (PGSTAT204, Metrohm) coupled by a Nova 2.1 software. All experiments were conducted using a standard three-electrode cell system. A BDD film was used as the working electrode, while a Pt wire and an Ag/AgCl system as the counter and the reference electrode, respectively. The electrolyte solution was phosphate buffer solution (PBS) pH 7.4.

2.2 Preparation of the working electrode

The BDD film was prepared using microwave-assisted chemical vapor deposition (CVD) technique on the surface of silicon wafer was used as the working electrode. The synthesis of BDD has been previously described (Fujishima, 2005; Suzuki et al., 2007). Methanol containing 1% trimethoxy boron together with hydrogen was used as the precursor materials. A deposition time of 8 hours in the CVD apparatus was applied. Raman spectroscopy used to evaluate the quality of BDD showed the spectrum with peaks at around 1333 cm^{-1}, indicated the presence of sp^3 C-C bonds of diamond (Nakamoto, 2008). In addition, the peak at 519 cm^{-1} was also observed to be correlated to the phonon excitation of boron (Fujishima, 2005). Besides Raman characterization, scanning electron microscope

(SEM) characterization was also performed, showing the formation of homogeneous crystals on the surface of Si wafer with the particle size of around 3 μm.

2.3 Immobilization of AChE with avidin-functionalized magnetic beads (AChE-aMB)

Prior to immobilizing AChE on aMB surface, AChE was modified with sulfo-NHS-biotin. Briefly, the solution of AChE in PBS was desalted using a PD-10 column, then mixed with sulfo-NHS-biotin solution before incubated for 1 hour at room temperature. The AChE-biotin adduct was stored at -200°C in PBS solution containing 50% glycerol and 1 mg/mL BSA. To activate the aMB, 30 μL aMB was washed by stirring in PBS (pH 7.6) before mixing with vortex. Then, aMB was separated from the solution and this washing step was repeated several times. The activated aMB was mixed with 50 μL AChE-biotin adduct solution with a gentle shaker for 5 minutes before incubated at 40°C for 12 hours and homogenized with vortex before placed in a magnetic holder. The separated aMB was washed with PBS to remove the undesired compounds, added with AChE-biotin adduct solution and incubated for 12 hours at 4 °C.

2.4 Electrochemical measurements of cholorpyrifos

Cyclic voltammetry (CV) applied over a potential range of -0.5 V to +1.5 V with an applied scan rate of 100 mV/s was used to optimize the electrochemical measurements. Preliminary studies were conducted to obtain the highest current response of ACTI. The pHs of ACTI solution in PBS varied from 6.8 to 7.5 while various ACTI concentrations were screened from $2x10^{-2}$ to 1 mM. A volume of 4.0 mL PBS (pH 7.4; 50 mM) was mixed with 0.5 mL ACTI (1.0 mM), then 0.5 mL of AChE (25 mU activity) was added. To obtain an optimum response, the contact time was varied from 0 to 30 minutes, while AChE concentration was varied from 5 to 50 mU.

In the electrochemical measurement using AChE-aMB, a magnetic bar was placed under BDD electrode. Initially, a solution containing 500 μL of 5 mM PBS (pH 7.6) and 100 μL of ACTI ($1x10^{-3}$ M) was mixed with 0.5 mL of 25 mU AChE before performing the electrochemical measurements and left in optimum time. Then, 100 μL chlorpyrifos was added with various concentrations from $1x10^{-5}$ to $1x10^{-1}$ mM was conducted and followed by 100 μL addition of AChE or AChE-aMB. The interference of metals was examined with 1 mL aliquot of the chlorpyrifos in water. The sample was added with 0.5 mL AChE or AChE-aMB before the addition of various concentrations of Fe or Mn ions.

3. Results and Discussion

3.1 Electrochemical behavior of thiocholine at BDD electrode

Voltammograms in Figure 1 indicate an oxidation reaction and a reduction reaction of thiocholine occur at the potential of 1.2 V and -0.3 V (vs. Ag/AgCl), respectively. This reaction is attributable to an enzymatic reaction of AChE, which acetylcholine was hydrolyzed into thiocholine and acetic acid (Figure 2). Since thiocholine is electroactive, the oxidation reduction reaction of thiocholine can be used to detect the AChE activity (Pino et al., 2015).

It is known that activity of enzyme is strongly dependent on the electrolyte. Most of enzymes show optimum activity in the pH range from 7.2 – 8.0 and below that range (pH around 5.0), the enzyme activity is decreased up to 70% (Carucci et al., 2017). To obtain the highest current response of ACTI, the pHs of ACTI solution in PBS varied from 6.8 to 7.5. Figure 1b shows that the highest current response could be detected at pH 7.4. Accordingly, this pH was selected for the next experiments. Further measurements performed using 50 mM PBS pH 7.4 containing various ACTI concentrations from $2x10^{-2}$ to 1 mM show the increase of oxidation currents along with the increase of ACTI concentration. Since the peak at 1.0 V is correlated to the presence of ACTI, increasing of ACTI concentrations results in

the increase of the peak intensity. Plots of the oxidation current responses of the voltammograms shows linear correlation against the concentrations (Figure 1c) in the range of $2x10^{-2}$ to 1 mM with a regression coefficient of 0.9879. The results suggest that the system can be applied for thiocholine detection.

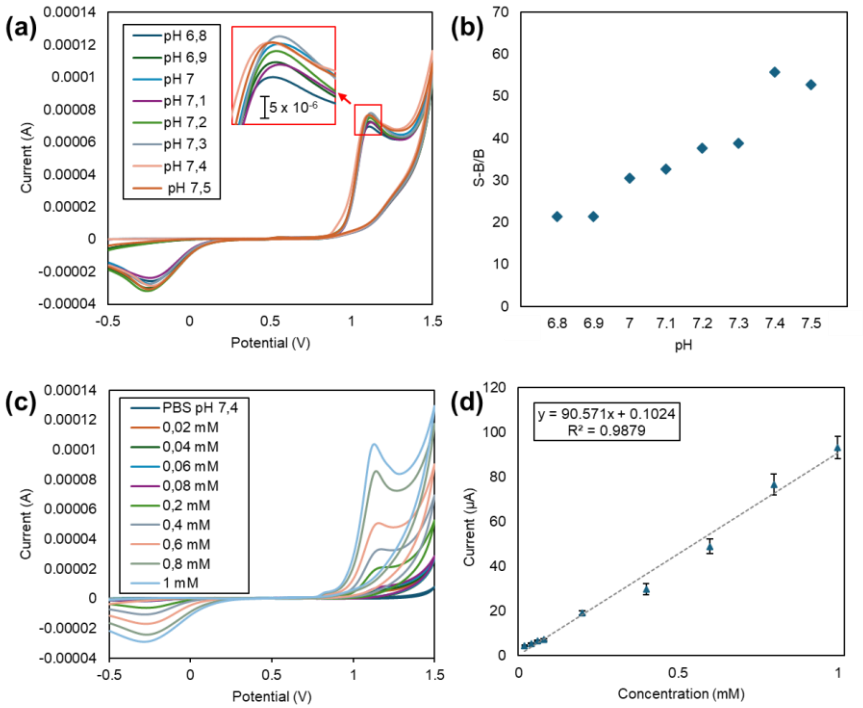

Fig. 1. Voltammograms of 0.1 M PBS containing 1 mM ACTI (a) in various pHs and (c) in various ACTI concentrations, and (b) and (d) showed the related signal-to-background current dependence on pH and linear regression curve, respectively

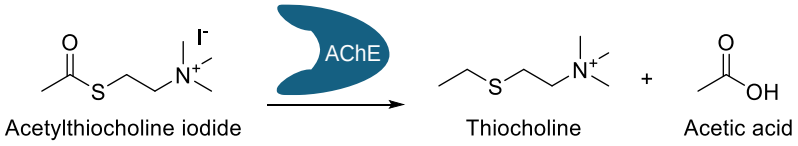

Fig. 2. Enzymatic hydrolysis of ACTI to produce thiocholine

To determine the optimum contact time between ACTI and AChE, the measurement was performed using PBS pH 7.4 and 25 mU/mL of AChE (Figure 3a). AChE peak was not observed until 15 minutes contact time. When the contact time was extended to 20 minutes, an AChE peak was observed around 0.8 V which has lower oxidation potential compared with the ACTI peak (1.0 V). Increasing the contact time to 25 minutes gave the highest current response, indicating the optimum contact time for AChE.

Enzyme activity can be influenced by several factors, including pH. It is known that enzyme has an optimal pH range. While enzyme activity becomes suboptimal below the optimal pH and denatures above it. AChE is known to reach an optimal activity in pH range between 7.2 and 8.0. Figure 3b and 3c show the voltammograms of 1 mM ACTI solution in 50 mM PBS at various pH from 7.2 to 7.7. The highest oxidation current of AChE was observed at pH 7.6, which is considered the optimal pH.

The measurements of AChE oxidation performed in 50 mM PBS pH 7.4 solution containing various AChE concentrations from 5 to 50 mU. The observed oxidation current at 0.8 V peak showed the good linearity against AChE concentrations (Figure 3d). However, the oxidation current response of the AChE 5 mU activity gave slightly small responses,

while from the 40 to 50 mU activity the oxidative current responses were shifted. The linear correlation between the current and AChE concentration were studied and finally obtained a regression coefficient of 0.9533. Based on the linearity result, LOD was calculated and obtained value of 15.5 mU. The result showed good tolerance with the small amount of AChE while using BDD electrode.

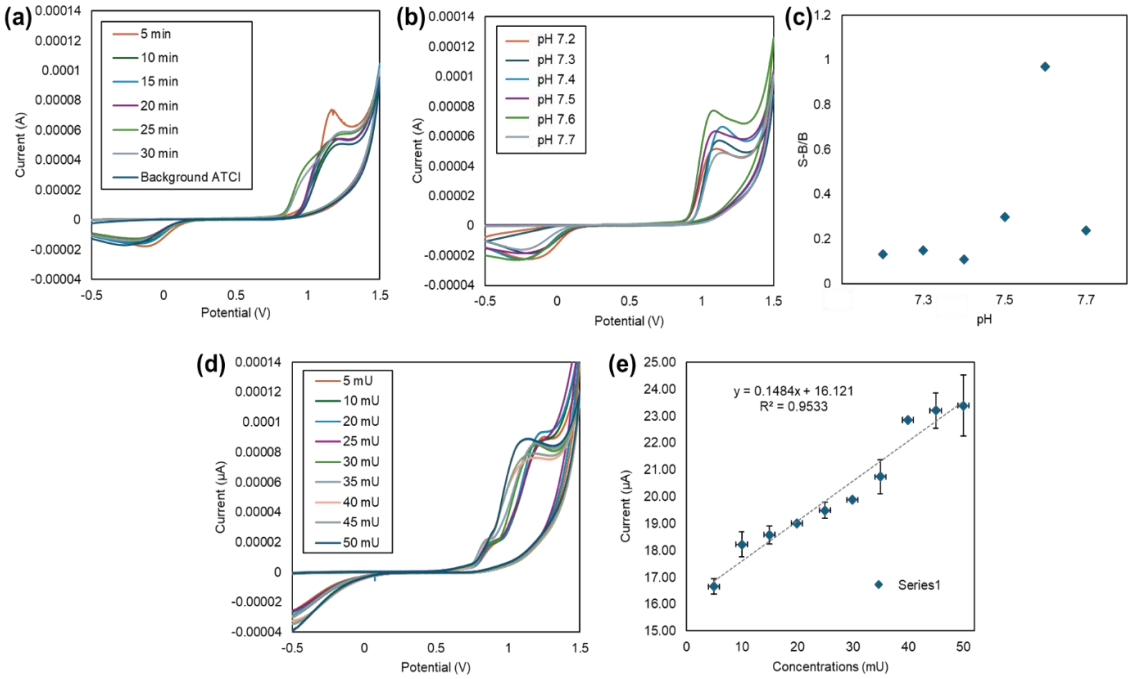

Fig. 3. Voltammograms of 0.1 M PBS containing 1 mM ACTI and 25 mU/mL AChE (a) and (b) in various contact times and (c) in various pHs together with (d) the related signal-to-background current dependence on pH. (e) Voltammograms of 0.1 M PBS containing 1 mM ACTI and various activity of AChE in pH 7.6 and (f) the related linear regression curve

3.2 AChE immobilization with aMB (AChE-aMB)

AChE was modified with sulfo-NHS-biotin before being immobilized with aMB. This step introduces biotin compound as a linker. However, the reaction can be interfered with the tris-buffer in AChE. Tris-buffer in AChE can compete with sulfo-NHS-biotin, since both molecules contain amine groups that reacts with the enzyme's binding sites (Usui et al., 2004). As a result, the initial step is to remove the tris-buffer with a PD-10 column.

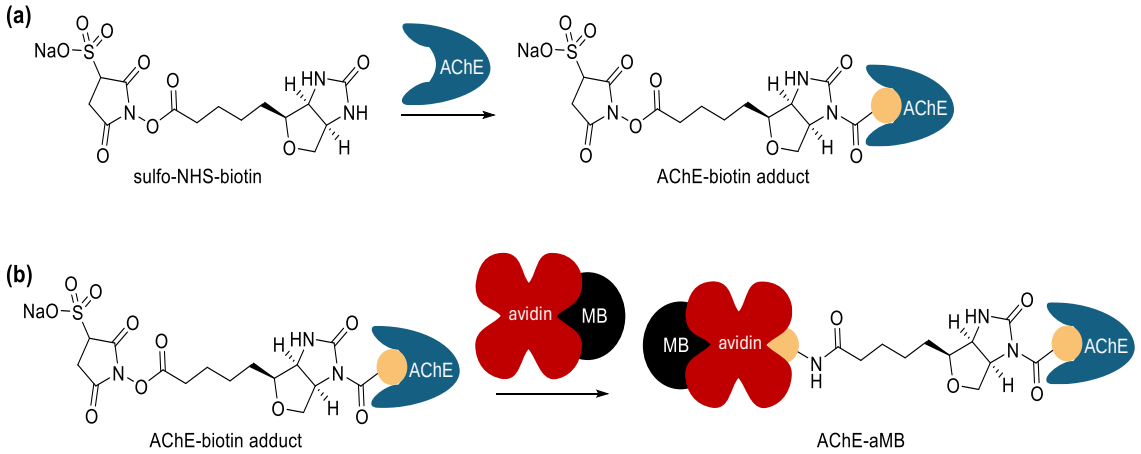

Fig. 4. The synthesis of (a) AChE-biotin adduct, (b) AChE-aMB.

The synthesis of AChE-biotin adduct was conducted through amide-formation reaction. The carboxylic site of AChE reacts with the cyclic amine group of sulfo-NHS-biotin, making amide bond as shown in Figure 4a. Despite the formation of amide bond between AChE and sulfo-NHS-biotin, a non-stable covalent or a hydrogen bond, were also observed. The resultant AChE-biotin adduct was stored at 4°C in a solution containing 50% glycerol, 1 mg/mL BSA, and 50 mM PBS to ensure the stability of the AChE-biotin adduct. Glycerol was used to prevent enzyme denaturation during storage at low temperature while BSA can prevent undesired reaction.

The next step was immobilization the AChE-biotin to the aMB. The reactive sites of each compound were amine group in aMB and sulfo-NHS ester in the AChE-biotin adduct (Figure 4b). The reaction is similar to the formation of AChE-biotin adduct, which formed the amide bond. The key step of this immobilization was the utilization of sulfo-NHS as a leaving group, made the amine group in aMB was easier to attack the carbonyl group in the NHS ester. The electrochemical performance of AChE-aMB was conducted with the help of magnetic bar. By putting magnetic bar under BDD electrode, the immobilization of AChE-aMB on BDD electrode was simply achieved with a good stability. This immobilized AChE sensor performance then compared with free AChE using BDD electrode.

3.3 Electrochemical performance of chlorpyrifos on AChE and AChE-aMB

The electrochemical performance of chlorpyrifos began with the optimization of inhibition time between AChE as the enzyme and chlorpyrifos as an inhibition as well as the concentration of chlorpyrifos. The inhibition time measures the optimum contact time. Linear sweep voltammetry (LSV) in a potential range from -0.5 V to +1.5 V was applied to obtain the optimum inhibition time (Figure 5a).

Thiocholine oxidation current response was not observed owing to the proximity of the thiocholine to the ACTI oxidation current response, leading to the overlap of two current peaks. Theoretically, the oxidation current of ACTI comes from the iodide ions oxidation (Fierro et al., 2013). From the voltammogram, the correlation between oxidative current response and contact time has been analyzed (Figure 5b). From 2 to 5 minutes, the oxidative current response increased. However, in 10 minutes it showed decrement of oxidative current response and tend to be stagnant afterwards. The optimum inhibition time was set at 10 minutes and will be used for the next optimization.

After that, the oxidation of thiocholine was performed using various AChE and AChE-aMB concentrations from $1x10^{-5}$ to $1x10^{-1}$ mM. The BDD electrode current response to the system will be proportionally inversed. A higher concentration of chlorpyrifos will result in a decrease of thiocholine oxidation current response. However, more amount blocks the active sites of AChE. The voltammograms carried out at the solution containing chlorpyrifos in the mixture of 25 mU/mL AChE and AChE-aMB was showed in Figure 5c and 5d, respectively.

The thiocholine oxidation current response was observed around 0.8 V. This peak was expected to be overlapped between thiocholine and ACTI peaks. AChE-aMB oxidative current response was smaller compared with AChE because the surface area of BDD was covered with aMB and prevents the electron transfer from the electrolyte to the electrode surface. The oxidation currents in Figure 5c and 5d were assumed to represent the oxidation of both thiocholine and ACTI. In that case, that peak has a similar effect on the individual thiocholine peak. To confirm this effect, the difference between the oxidation currents response was calculated with and without chlorpyrifos, then plotted against the chlorpyrifos concentration, as shown in Figures 5e. The calibration curve shows that the chlorpyrifos concentration is proportional to the % inhibition. From the calibration curve, the slope of AChE is greater than that of AChE-aMB, suggesting that the AChE is more sensitive than AChE-aMB in the detection of chlorpyrifos pesticide.

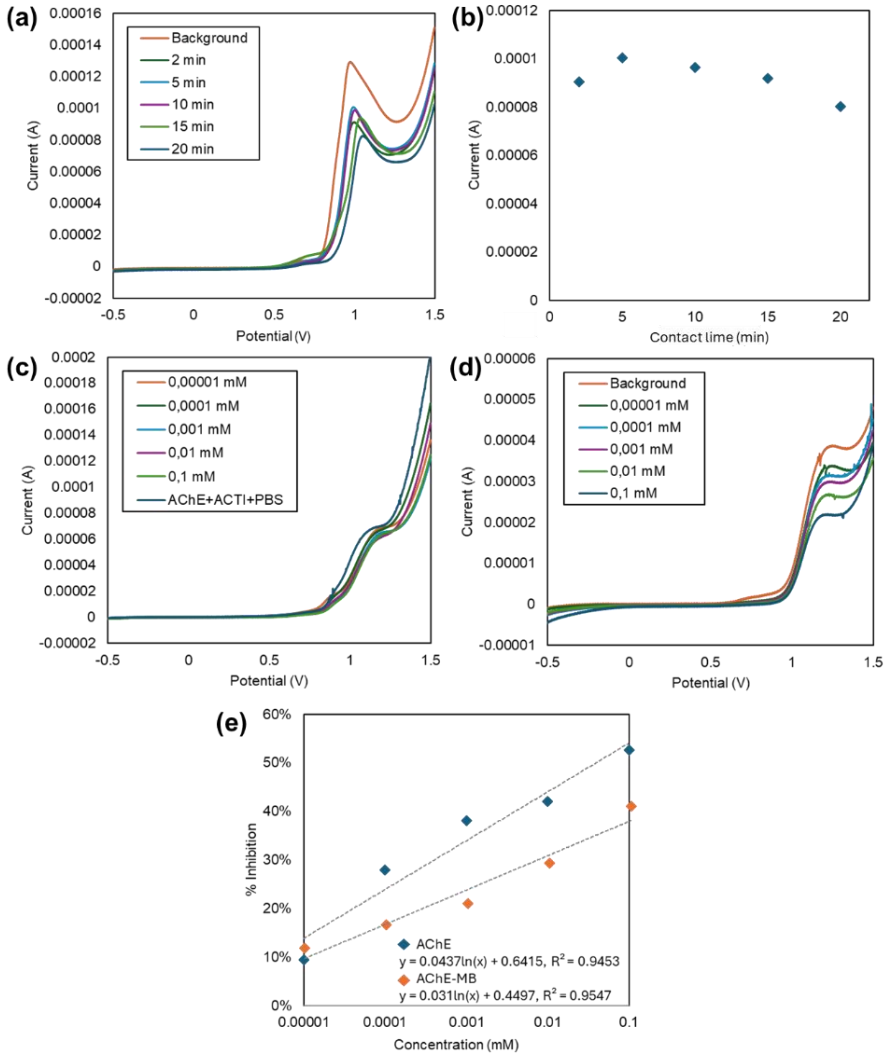

Fig. 5. Voltammograms of 0.1 M PBS and 1 mM ATCI containing 1 mM chlorpyrifos pesticide and 25 mU/mL AChE (a) and (b) in various contact time, (c) and (d) in various chlorpyrifos pesticide concentration in AChE and AChE-aMB, respectively. (e) show the linear regression curve

The inhibition percentage was calculated from the oxidation current before and after the addition of chlorpyrifos (Table 1). The values IC_{10} and IC_{50} indicate the inhibitory concentrations at 10% and 50%, respectively. The results showing around 4 times lower inhibitory concentrations of IC_{10} of AChE ($3.435x10^{-6}$ mM) than AChE-aMB (12.9x10-6 mM) and around 2 orders lower of IC_{50} of free AChE ($3.8x10^{-4}$ mM) than the immobilized AChE (5.18 mM). The immobilization of AChE onto aMB still gives higher IC_{10} and IC_{50} values compared to the free AChE although the stability of AChE-aMB on BDD surface is better than free AChE.

Table 1 Inhibitory concentration of chlorpyrifos on AChE and AChE-aMB

Concentration (mM)	% Inhibition	
	AChE	AChE-aMB
0.00001	9.37	11.33
0.0001	27.89	16.18
0.001	38.03	20.31
0.01	42.04	28.92
0.1	52.57	40.68
IC_{10}	$3.44x10^{-6}$ mM	$12.9x10^{-6}$ mM
IC_{50}	$3.8x10^{-4}$ mM	5.18 mM

3.4 Interference Study on AChE and AChE-aMB

The interference of metal ions was examined using Fe^{2+} and Mn^{2+} added into the electrochemical system. LSV was conducted over a potential range of -0.5 to 1.5 V in various the concentrations of Fe^{2+} and Mn^{2+} ions between $5x10^{-4}$ to $5x10^{-3}$ µM. The voltammograms (Figure 6a and 6b) show the oxidation current response decrease with the increase of metal ion concentration. Metal ions can inhibit the enzyme activity by binding to the enzyme's active site. The inhibition effect of metal ions on the pesticides detection was examined for each enzyme in the electrochemical system. At free AChE, Fe^{2+} ion addition gave the lower oxidative current response of thiocholine since the Fe^{2+} ion has a stronger binding affinity to the enzyme's active site compared with Mn^{2+} ion. As a result, Fe^{2+} gave higher signal loss percent in each concentration compared with Mn^{2+} (Table 2).

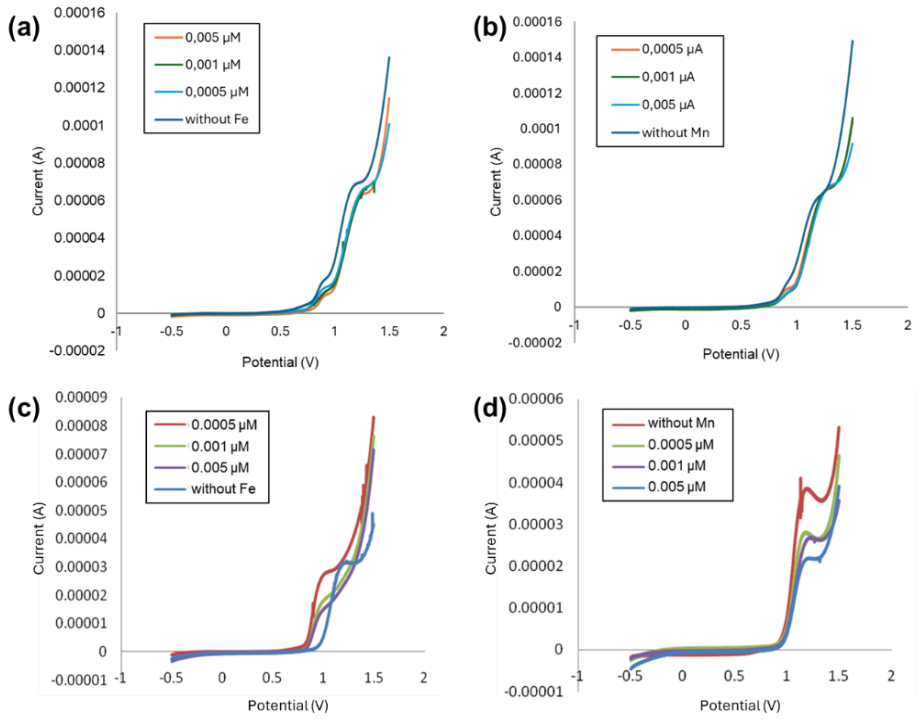

Fig. 6. Voltammograms of 50 mM PBS and 10 mM ATCI containing the mixture of chlorpyrifos pesticide with AChE and (a) Fe^{2+} ion, (b) Mn^{2+} ion, the mixture of chlorpyrifos pesticide with AChE-aMB and (c) Fe^{2+} ion, (d) Mn^{2+} ion

The effect of the metal ion interference was also studied on AChE-aMB. Figure 6c and 6d are the voltammograms of AChE-aMB with Fe^{2+} and Mn^{2+} as metal ion interferences. From the voltammogram, it can be observed that the higher concentration of metal ion will give similar trend with AChE results. On the contrary, the smallest concentration of Fe^{2+} ion interference ($5x10^{-4}$ µM) showed a peak shifting in the AChE-aMB compared to the control (without Fe^{2+} ion). It could be affected by the nanoparticles presented in the aMB sites. As shown in Table 2, the presence of aMB could give low signal loss percent ($5x10^{-4}$ µM Fe^{2+}, 15.4% signal loss) while Mn^{2+} gave higher signal loss percent ($5x10^{-4}$ µM Mn^{2+}, 29.5% signal loss).

Table 2. Percentage of the signal reduction of the systems with free AChE and AChE-aMB in the presence of Fe^{2+} and Mn^{2+} as interferences

Concentration	Free AChE (%)		Immobilized AchE (%)	
(mM)	Fe	Mn	Fe	Mn
0.5	23.6	13.8	15.4	29.5
1.0	37.0	37.5	44.3	32.8
5.0	48.7	40.8	53.9	45.9

The immobilization of AChE-aMB was also studied to determine the efficiency of the chlorpyrifos sensor system. Modification with magnetic beads were known to enhance the stability and the performance of the sensor. The utilization of magnetic beads can facilitate the electron transfer more efficiently and simply attract the magnetic bioconjugate using the magnet located under the electrode. In this metal ion interference studies, only low concentration of Fe^{2+} (5x10-4 uM) give satisfactory result. Conversely, AChE-aMB in this study has higher affinity to metal ions due to the presence of Fe nanoparticles in the magnetic beads. Overall it can be concluded that the system with free AChE exhibits a greater resistance to the interference of metal ions than that of immobilized AChE-aMB.

4. Conclusions

The investigation of the chlorpyrifos sensor has been performed using BDD surface between free acetylcholinesterase (AChE) and AChE-modified on magnetic beads (AChE-aMB). The linear calibration curve on the optimum contact time and pH could be achieved over a concentration range of from $1x10^{-1}$ to $1x10^{-5}$ mM, with a regression coefficient of 0.945. The IC_{10} and IC_{50} shows the good inhibitory concentration of 10% and 50%, respectively, with free AChE (IC_{10} and IC_{50}; $3.44x10^{-6}$ mM and $3.8x10^{-4}$, respectively). Moreover, the effect of metal ion could cause a decrease in percent signal intensity. For the AChE-aMB, the percent signal loss decreased to 15.4% for Fe^{2+}. While another metal ions and bigger concentration resulted in undesired data. The immobilization of AChE-aMB is still promising system to be used in sensor and the continuity of this research is necessary in the future. Finally, to develop a highly sensitive sensor, it is essential to remove all interfering substances and suggested that careful immobilization has to be considered while immobilizing AChE for the sensor application.

Acknowledgement
The authors sincerely thank the Department of Chemistry, Faculty of Mathematics and Science, Universitas Indonesia for their support in this research. The authors also appreciate the valuable insights from colleagues and reviewers, which have significantly contributed to the enhancement of this manuscript. Their guidance and constructive feedback are greatly acknowledged.

Author Contribution
All authors contributed equally to the conceptualization, methodology, analysis, and writing of this review. They collaboratively reviewed and approved the final manuscript for submission.

Funding
This research received no external funding.

Ethical Review Board Statement
Not available.

Informed Consent Statement
Not available.

Data Availability Statement
Not available.

Conflicts of Interest
The authors declare no conflict of interest.

Open Access

©2024. The author(s). This article is licensed under a Creative Commons Attribution 4.0 International License, which permits use, sharing, adaptation, distribution and reproduction in any medium or format, as long as you give appropriate credit to the original author(s) and the source, provide a link to the Creative Commons license, and indicate if changes were made. The images or other third-party material in this article are included in the article's Creative Commons license, unless indicated otherwise in a credit line to the material. If material is not included in the article's Creative Commons license and your intended use is not permitted by statutory regulation or exceeds the permitted use, you will need to obtain permission directly from the copyright holder. To view a copy of this license, visit: http://creativecommons.org/licenses/by/4.0/

References

Camacho, M., Alsford, S., & Agnew, A. (1996). Molecular forms of tegumental and muscle acetylcholinesterases of *Schistosoma*. *Parasitology*, *112*(2), 199–204. https://doi.org/10.1017/S0031182000084766

Carucci, C., Salis, A., & Magner, E. (2017). Electrolyte effects on enzyme electrochemistry. *Current Opinion in Electrochemistry*, *5*(1), 158–164. https://doi.org/10.1016/j.coelec.2017.08.011

Chaplin, B. P., Hubler, D. K., & Farrell, J. (2013). Understanding anodic wear at boron doped diamond film electrodes. *Electrochimica Acta*, *89*, 122–131. https://doi.org/10.1016/j.electacta.2012.10.166

Chen, Y., Gao, X., Liu, G., Zhu, R., Yang, W., Li, Z., Liu, F., Zhou, K., Yu, Z., Wei, Q., & Ma, L. (2022). Correlation of the role of boron concentration on the microstructure and electrochemical properties of diamond electrodes. *Functional Diamond*, *1*(1), 197–204. https://doi.org/10.1080/26941112.2021.2017759

Fierro, S., Comninellis, C., & Einaga, Y. (2013). Simultaneous detection of iodine and iodide on boron doped diamond electrodes. *Talanta*, *103*, 33–37. https://doi.org/10.1016/j.talanta.2012.10.002

Fujishima, A. (2005). *Diamond electrochemistry*. Elsevier, Amsterdam.

Girard, H., Simon, N., Ballutaud, D., Herlem, M., & Etcheberry, A. (2007). Effect of anodic and cathodic treatments on the charge transfer of boron doped diamond electrodes. *Diamond and Related Materials*, *16*(2), 316–325. https://doi.org/10.1016/j.diamond.2006.06.009

Hernández, F., Sancho, J. V., & Pozo, O. J. (2005). Critical review of the application of liquid chromatography/mass spectrometry to the determination of pesticide residues in biological samples. *Analytical and Bioanalytical Chemistry*, *382*(4), 934–946. https://doi.org/10.1007/s00216-005-3185-5

Mishra, A., Kumar, J., Melo, J. S., & Sandaka, B. P. (2021). Progressive development in biosensors for detection of dichlorvos pesticide: A review. *Journal of Environmental Chemical Engineering*, *9*(2), 105067. https://doi.org/10.1016/j.jece.2021.105067

Nakamoto, K. (2008). *Infrared and Raman Spectra of Inorganic and Coordination Compounds*. Wiley. https://doi.org/10.1002/9780470405840

Nandhini, A. R., Harshiny, M., & Gummadi, S. N. (2021). Chlorpyrifos in environment and food: a critical review of detection methods and degradation pathways. *Environmental Science: Processes & Impacts*, *23*(9), 1255–1277. https://doi.org/10.1039/D1EM00178G

Pico, Y., Alfarhan, A. H., & Barcelo, D. (2020). How recent innovations in gas chromatography-mass spectrometry have improved pesticide residue determination: An alternative technique to be in your radar. *TrAC Trends in Analytical Chemistry*, *122*, 115720. https://doi.org/10.1016/j.trac.2019.115720

Pino, F., Tribidasari A., I., Nakata, K., Fujishima, A., Merkoçi, A., & Einaga, Y. (2015). Magnetic Enzymatic Platform for Organophosphate Pesticide Detection Using Boron-doped Diamond Electrodes. *Analytical Sciences*, *31*(10), 1061–1068. https://doi.org/10.2116/analsci.31.1061

Rachmawati, A., Sanjaya, A. R., Putri, Y. M. T. A., Gunlazuardi, J., & Ivandini, T. A. (2023). An acetylcholinesterase-based biosensor for isoprocarb using a gold nanoparticles-polyaniline modified graphite pencil electrode. *Analytical Sciences*, *39*(6), 911–923. https://doi.org/10.1007/s44211-023-00296-7

Raharto, T., Setiyanto, C. M., Ariyanta, H. A., Nahda, D. P. N., Hani, A. M., Yulizar, Y., & Ivandini, T. A. (2023). Synthesis of gold nanoparticles with allicin to modify boron-doped diamond surface for oxygen sensor applications. *Environmental and Materials*, *1*(2). https://doi.org/10.61511/eam.v1i2.2023.560

Suzuki, A., Ivandini, T. A., Yoshimi, K., Fujishima, A., Oyama, G., Nakazato, T., Hattori, N., Kitazawa, S., & Einaga, Y. (2007). Fabrication, Characterization, and Application of Boron-Doped Diamond Microelectrodes for in Vivo Dopamine Detection. *Analytical Chemistry*, *79*(22), 8608–8615. https://doi.org/10.1021/ac071519h

Usui, K., Ishii, N., Kawarabayasi, Y., & Yohda, M. (2004). Expression and biochemical characterization of two small heat shock proteins from the thermoacidophilic crenarchaeon *Sulfolobus tokodaii* strain 7. *Protein Science*, *13*(1), 134–144. https://doi.org/10.1110/ps.03264204

Van Dyk, J. S., & Pletschke, B. (2011). Review on the use of enzymes for the detection of organochlorine, organophosphate and carbamate pesticides in the environment. *Chemosphere*, *82*(3), 291–307. https://doi.org/10.1016/j.chemosphere.2010.10.033

Vosáhlová, J., Koláčná, L., Daňhel, A., Fischer, J., Balintová, J., Hocek, M., ... & Fojta, M. (2018). Voltammetric and adsorption study of 4-nitrophenyl-triazole-labeled 2′-deoxycytidine and 7-deazaadenosine nucleosides at boron-doped diamond electrode. *Journal of Electroanalytical Chemistry, 821,* 111-120. https://doi.org/10.1016/j.jelechem.2018.01.003

Waldvogel, S. R., & Elsler, B. (2012). Electrochemical synthesis on boron-doped diamond. *Electrochimica Acta*, *82*, 434–443. https://doi.org/https://doi.org/10.1016/j.electacta.2012.03.173

Wołejko E, Łozowicka B, Jabłońska-Trypuć A, Pietruszyńska M, Wydro U. (2022). Chlorpyrifos Occurrence and Toxicological Risk Assessment: A Review. *International Journal of Environmental Research and Public Health*; *19*(19), 12209. https://doi.org/10.3390/ijerph191912209

Biographies of Authors

Shafrizal Rasyid Atriardi, Chemistry Institute for Functional Material, Pusan National University, Busan, 46241, Republic of Korea.

- Email: shafrizalrasyid@pusan.ac.kr
- ORCID: 0000-0001-5797-3741
- Web of Science ResearcherID: N/A
- Scopus Author ID: 57209224198
- Homepage: N/A

Adinda Muthia Hani, Department Chemistry, Faculty of Mathematics and Natural Sciences, Universitas Indonesia, Depok, West Java 10430, Indonesia.

- Email: adinda.muthia@ui.ac.id
- ORCID: N/A
- Web of Science ResearcherID: N/A
- Scopus Author ID: N/A
- Homepage: N/A

Gadis Putri, Department Chemistry, Faculty of Mathematics and Natural Sciences, Universitas Indonesia, Depok, West Java 10430, Indonesia.

- Email: gadis.putri23@rocketmail.com
- ORCID: N/A
- Web of Science ResearcherID: N/A
- Scopus Author ID: N/A
- Homepage: N/A